

Research Article

INTERNATIONAL JOURNAL OF ADVANCED ROBOTIC SYSTEMS

International Journal of Advanced Robotic Systems March-April 2018: I – 10 © The Author(s) 2018 DOI: 10.1177/1729881418765884 journals.sagepub.com/home/arx



The maximum output force controller and its application to a virtual surgery system

Lingyan Hu¹, Jianhua Li¹, Xiaoping Liu², Pengwen Xiong¹ and Shengxing He¹

Abstract

It is difficult to achieve ideal virtual surgery transparency and stability when virtual tissue stiffness and damping are high. Typically, the stability of the surgery system is improved, while its transparency is sacrificed. In order to achieve high transparency in virtual surgical interactions, a maximum output force controller based on passive theory is proposed in this work. This controller is then applied in a virtual surgery system. The maximum output force controller predicts the maximum allowable output force above which the system passivity is broken and limits the force presented to the operator to this amount. The main contributions of this work include the following two parts: firstly, the maximum output force controller is developed and applied to a virtual surgery system; secondly, a new criterion for transparency is presented and analyzed for the level of transparency that can be achieved for a virtual surgical system when the stability is guaranteed. Experimental results show that the maximum output force controller can guarantee stability of the virtual surgical interaction with maximum transparency even when the virtual tissue stiffness and damping are high. In addition, the maximum output force controller is a self-adaptive controller. It works well without modification, regardless of the virtual tissue stiffness and damping.

Keywords

Virtual surgery, stability, maximum output force controller, transparency

Date received: 30 May 2017; accepted: 21 January 2018

Topic: Al in Robotics; Human Robot/Machine Interaction

Topic Editor: Arianna Menciassi Associate Editor: Yukio Takeda

Introduction

Over the past few decades, virtual surgery has developed rapidly with advancements in computing technology. Virtual surgery systems have been developed to reduce risk during surgeon training. A surgeon using a virtual surgery system can both see virtual interactions between tissues and surgical instruments and feel force feedback via a haptic device. Previous research has focused on visual feedback. The introduction of force feedback can cause system instability. However, haptic feedback plays an important role during a virtual surgery, because surgeons often rely on tactile and kinesthetic sensations during complex operations. As such, researchers have recently started to focus on haptic feedback research.

Force feedback has both positive and negative attributes. It enhances operator performance and allows surgeons to experience an immersive environment during surgery.^{3,4} However, it negatively influences system stability, especially when virtual tissues are rigid.

Corresponding author:

Pengwen Xiong, School of Information and Engineering, Nanchang University, 999 Xuefu Road, Nanchang 330031, China. Email: steven.xpw@ncu.edu.cn

School of Information and Engineering, Nanchang University, Nanchang,

² Department of Systems and Computer Engineering, Carleton University, Ottawa, ON, Canada

To solve the above problem, there has been significant research on passivity theorem, because it is an established framework for analyzing system stability. Colgate et al.⁵ introduced the idea of a virtual coupling that guarantees stability for arbitrary passive human operators and environments. Virtual coupling can restrict the impedance required by a virtual environment to such a level that stable haptic interactions can be guaranteed. However, the virtual coupling cannot guarantee stability in active environments. Adams and Hannaford derived the concept of a virtual coupling based on a two-port network. The criteria for unconditional stability proposed by Llewelyn was introduced as a tool for the design and evaluation of virtual coupling networks. However, it is very difficult to optimize virtual coupling parameters for performance. One must identify physical damping parameters through a complex dynamic characterization of the haptic interface, which is especially difficult in the case of a multipledegrees of freedom (DOF) haptic device. Kim and Ryu proposed a novel energy-bounding algorithm.7 The proposed energy-bounding algorithm restricted the energy generated by the sampler and human operator to the consumable energy by placing physical damping elements in the virtual environment. It considered only system stability and neglected system transparency.

Hannaford and Ryu defined a passivity observer (PO) and a passivity controller (PC) and proposed the PO/PC algorithm as a method of guaranteeing system stability. The PO was used to measure the energy flow in and out of one or more subsystems in real-time software. Active behavior was indicated by a negative PO value. The PC could be used at any sampling instant to accurately measure absorption of the PO network energy output and ensure system stability. These methods can be applied to environments with high stiffness; however, the PO/PC algorithm is limited to a fixed virtual environment. It needs to calculate the specific energy consumption element of the value to offset the leakage energy and maintain system passivity.

Recently, Ryu and Yoon proposed the memory-based passivation approach (MBPA), a new passivation method designed to increase the impedance range in which a haptic interface can passively interact in high-stiffness virtual environments. This technology was implemented using a six-DOF haptic device and exhibited better performance than the recently proposed field-programmable gate array-based time-domain passivity approach. However, the MBPA assumes that position resolution is uniform in all directions and, thus, is not easy to implement.

In order to maximize system fidelity, Kyungno and Doo presented an adjusting output-limiter (AOL) for stable haptic rendering in virtual environments. ¹⁴ The AOL maximized the system fidelity and guaranteed system passivity. However, the study included only a simulation in a generally deformable virtual environment, and system transparency was not discussed in detail.

Inspired primarily by the ideas presented in the literature, 14 this article develops a maximum output force controller (MOFC) for virtual surgical interactions. The MOFC observes the energy flow in system at every sampling instant. It predicts the maximum allowable output force at the next sampling instant in order to guarantee system passivity and limits the actual output force to this value. Thus, the system can offer maximum fidelity while guaranteeing stability. The actual experimental results show that the MOFC can achieve a stable interaction, regardless of virtual tissue stiffness and damping. The virtual surgical instrument can move along the expected trajectory stably during rigid interactions with the MOFC, while the same interactions are unstable without the MOFC. The main contribution of this article exists in the following two facts: firstly, the MOFC is developed and applied to a virtual surgery system; secondly, a new criterion for transparency is presented and is analyzed for the level of transparency that can be achieved for a virtual surgical system when the stability is guaranteed, which is not available in previous works.

The remainder of the article is organized as follows. The second section illustrates why virtual surgery systems are nonpassive, the third section gives the details of the algorithm developed. Application of the MOFC to virtual surgery is introduced in the fourth section. The fifth section presents a new criterion for transparency of a haptic interaction system. Experimental results are presented in the sixth section, followed by concluding remarks and recommendations for future work in the final section.

Nonpassivity of the virtual surgery system

Passivity is a sufficient condition for stability. Thus, if a system is passive, it must be stable. The unique advantage of using passivity theory to design a controller for interconnected systems is its closure property, which implies that a combination of two or more passive systems connected in either feedback or parallel form is also passive. In order to analyze the system passivity, the virtual surgery system can be decomposed into four interconnected subsystems: an operator, a haptic device, a sampler and holder, and a virtual environment, as shown in Figure 1.15 An operator holds a haptic device and moves with velocity $v_o(t)$. The haptic device is mapped to a virtual instrument and interacts with virtual tissues. The velocity of the haptic device (virtual instrument) is $v_h(t)$. After discretization, the velocity of the virtual instrument at the kth sampling instant is $v_e(k)$. $f_e(k)$ is the force of interaction between the virtual instrument and virtual tissues according to the virtual model, while $f_h(t)$ is the continuous interaction force and $f_o(t)$ is the output force presented to the operator.

Definition⁸: The two-port network shown in Figure 2 with initial energy storage $E(\theta)$ is passive, if and only if

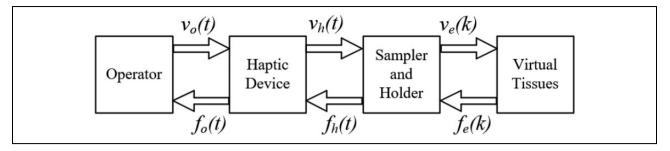


Figure 1. The two-port network of the virtual surgery system.

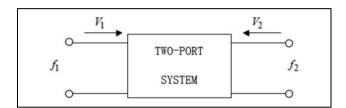


Figure 2. Two-port network.

$$\int_{0}^{t} \left(f_{1}(\tau) v_{1}(\tau) + f_{2}(\tau) v_{2}(\tau) \right) dt + E(0) \ge 0, \forall t \ge 0 \quad (1)$$

for force (f_1, f_2) and velocities (v_1, v_2) , where t is the time variable.

Thus, the energy supplied to a passive network must be greater than negative $E(\theta)$ at all times. For the haptic interaction system shown in Figure 1, most previous research has considered the operator and the virtual tissues to be passive, 16,17 and the haptic device itself is also passive. 17 A virtual surgery system becomes nonpassive because of the sampler and holder. The sampler and holder represent a sampled data system whose energy is expressed in equation (2)

$$E(n) = \int_0^{nT} f_h(t) v_h(t) dt - T \sum_{k=0}^{n-1} f_e(k) v_e(k)$$
 (2)

For a zero-order holder, equation (3) can be derived as in Kim and Ryu's work⁷

$$E(n) = \sum_{k=0}^{n-1} \int_{kT}^{(k+1)T} f_h(t) v_h(t) dt - T \sum_{k=0}^{n-1} f_e(k) v_e(k)$$

$$= \sum_{k=0}^{n-1} f_e(k) \int_{kT}^{(k+1)T} v_h(t) dt - T \sum_{k=0}^{n-1} f_e(k) v_e(k)$$

$$= \sum_{k=0}^{n-1} f_e(k) (x(k+1) - x(k)) - T \sum_{k=0}^{n-1} f_e(k) v_e(k) \quad (3)$$

Therefore, the energy cannot be predicted perfectly, because it contains future position x(k+1) and x(k). They may be negative or not. The sampler and holder may

generate energy to the system and destroy the overall system passivity.

MOFC algorithm

The above analysis shows that the sampler and holder may generate energy to the system leading to system instability. Therefore, the key to ensuring system passivity is to design a controller that keeps the sample and holder passive. Based on Kyungno and Doo's study,14 we developed an MOFC for a virtual surgical interaction system, as shown in Figure 3. We named the combined subsystem, including the haptic device, sample and holder, MOFC, and virtual tissues, "HSME." The purpose of the MOFC is to keep the HSME passive.

The MOFC ensures that the total energy of the HSME satisfies the conditions for passivity, making the overall system stable. The MOFC observes the energy of the HSME at every sampling instant. It monitors and analyzes the input and output energies, then predicts the maximum allowable output force at the next sampling instant in order to keep the HSME passive. If the actual output force presented to the operator is limited to the maximum allowable value, the HSME is certain to be passive, and thus the entire virtual surgery system is passive. The details of the MOFC design follow.

The maximum output force

For the virtual surgery system with a two-port network shown in Figure 3, we define that the product of force and velocity is positive when energy flows from the system. We consider the energy $E_{\rm hsme}(k)$ of the HSME. The total energy $E_{\rm hsme}(k)$ from sampling instant 0 to kT is described by equation (4)

$$E_{\text{hsme}}(k) = E_h(k) + E_s(k) + E_e(k)$$
 (4)

where T is the sampling period, $E_h(k)$ is the total energy in the haptic device, $E_s(k)$ is the total energy in the sampler and holder, and $E_e(k)$ is the sum of the total energies in the MOFC and virtual tissues. The following equations can be derived according to Kyungno and Doo¹⁴

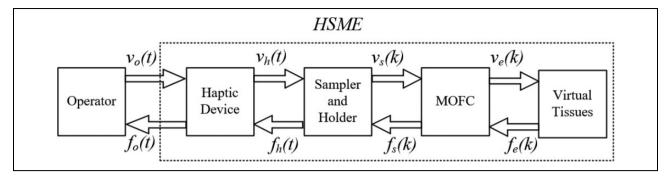


Figure 3. The two-port network of the virtual surgery system with the MOFC. MOFC: maximum output force controller.

$$E_h(k) \ge f_d T \sum_{n=0}^{k-1} v_s(n+1)^2 + f_{co} T \sum_{n=0}^{k-1} |v_s(n+1)|$$
 (5)

$$E_s(k) = T \sum_{n=0}^{k-1} f_s(n) \, v_s(n+1) - T \sum_{n=0}^{k-1} f_s(k) \, v_s(k)$$
 (6)

$$E_e(k) = T \sum_{n=0}^{k-1} f_s(k) v_s(k)$$
 (7)

$$E_{\text{hsme}}(k) \ge E'_{\text{hsme}}(k) = f_d T \sum_{n=0}^{k-1} v_s (n+1)^2$$

$$+ f_{co} T \sum_{n=0}^{k-1} |v_s(n+1)| + T \sum_{n=0}^{k-1} f_s(n) v_s (n+1)$$
(8)

The minimum Coulomb friction $f_{\rm co}$ and damping friction $f_{\rm d}$ in equations (5) to (8) are inherent to the environment and can be calculated based on the work by Kyungno and Doo.¹⁴

The total energy $E_{\text{hsme}}(k+1)$ of the HSME from sampling instant 0 to sampling instant (k+1)T is

$$E_{\text{hsme}}(k+1) = E_{\text{hsme}}(k) + e(k+1)$$
 (9)

where e(k+1) is the energy of the HSME at instant (k+1)T, which is the energy in the independent point of the subsystem

$$e(k+1) = f_d T v_s(k+1)^2 + f_{co} T \operatorname{sgn}(v_s(k+1)) v_s(k+1) + T f_s(k) v_s(k+1)$$

$$\operatorname{sgn}(x) = \left\{ \begin{array}{cc} 1, & x > 0 \\ 0, & x = 0 \\ -1, & x < 0 \end{array} \right\}$$
 (10)

then

$$E_{\text{hsme}}(k+1) \ge E'_{\text{hsme}}(k) + f_d T v_s (k+1)^2 + T f_{so} \operatorname{sgn}(v_s(k+1)) v_s(k+1) + T f_s(k) v_s(k+1)$$
(11)

To ensure that the system is passive, we must ensure that $E_{\text{hsme}}(k+1) \ge 0$ at all times. The minimum velocity

required to minimize E(k+1) can be derived by differentiating equation (11).

$$v_s(k+1)_{\min} = -\left(f_s(k)\right) + \left(f_{co} \operatorname{sgn} v_s(k+1)\right) / 2f_d$$
 (12)

Based on equations (11) and (12), and the condition $E_{\text{hsme}}(k+1) \ge 0$, we can conclude that the haptic system is passive at (k+1)T, if equation (13) is satisfied:

$$-f_{co} - 2\sqrt{\frac{f_d \times E'_{hsme}(k)}{T}} \le f_s(k) \le f_{co} + 2\sqrt{\frac{f_d \times E'_{hsme}(k)}{T}}$$

$$f_{\text{max}} = f_{co} + 2\sqrt{\frac{f_d \times E'_{hsme}(k)}{T}}$$
 (13)

where f_{max} is the maximum allowable output force for guaranteed system passivity.

The actual output force

From the above equations, we can predict the maximum allowable output force that can guarantee system passivity at every sampling instant. The actual feedback force presented to the operator is corrected based on this maximum output force. The detailed correcting algorithm is presented in equation (14):

$$f_s(k) = \begin{cases} sgn(f_e(k)) f_{max} |f_e(k)| \ge f_{max} \\ f_e(k) |f_e(k)| < f_{max} \end{cases}$$
(14)

In summary, we predict the maximum allowable output force using equation (13) in order to guarantee that the HSME remains passive. If the HSME is passive, the entire virtual surgery interaction system is passive. The output force presented to the operator is then corrected using equation (14). When the interaction force calculated based on the virtual model is less than the maximum allowable force in the current sampling instant, the force is presented to the operator directly and system fidelity is ideal. When the virtual model interaction force is greater than the maximum allowable force, the virtual surgery interaction system will become active and unstable if the force is output directly without modification. So the output force presented to the

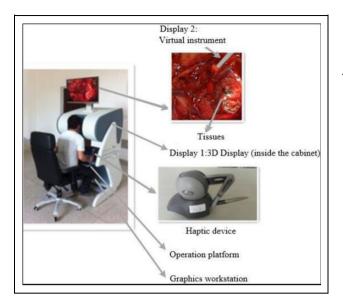


Figure 4. Virtual surgery system.

operator should be limited to the maximum allowable value in order to maintain system stability.

A virtual surgery system with an MOFC

We built a virtual surgery system with high immersion and fidelity as shown in Figure 4 and applied the MOFC to it. The system consists of two display devices, a mainframe, a haptic device, and a graphics workstation. The first display is in a cabinet with two pinholes through which an operator can see a three-dimensional (3-D) interaction scene. This provides a high degree of immersion to the operator. The second display is a normal two-dimensional display on the top. Two haptic devices can be placed on an operation platform (only a PHANTOM OMNI is used in this article). We built virtual models (including geometric and physical models) for the tissues and surgical instrument in a graphics workstation with an Intel Xeon E5-2630(v3) CPU and a NVIDIA Quadro K5200, to provide sufficiently fast computing. We used octree to organize the point cloud data of virtual tissues. The geometric model describes geometric information and topological relation of tissues. With the physical model, the interaction force between the virtual instrument and virtual tissues can be calculated and presented to the operator through the haptic device. The position of the six-DOF haptic device is mapped to that of the virtual surgical instrument during surgical interactions. Thus, the operator can hold the haptic device and control the virtual instrument during the operation. When the operator holds the haptic device and interacts with the virtual tissues, the deformation and interaction force can be calculated and presented based on the geometric and physical models. Therefore, the operator can see tissue deformation and feel interaction force between the surgical instrument and the virtual tissues with high immersion and fidelity.

The MOFC is applied to the virtual surgery system to ensure system stability. First, we read the haptic device position and velocity and calculate the interaction force $f_e(k)$ between the virtual tissues and the surgical instrument. Second, the total HSME energy is calculated at sampling instant kT. Third, we predict the total energy at the next instant and calculate the maximum allowable force f_{max} for guaranteed system passivity using equation (13). After comparing the interaction force $f_e(k)$ and the maximum allowable force f_{max} , the corrected output force $f_s(k)$ calculated based on equation (14) is presented to the operator through the haptic device. The primary virtual surgical interaction flowchart is shown in Figure 5.

Definition of transparency for a haptic interaction system

Transparency is used to quantify the performance as to how close the force presented to the operator is to that calculated by the virtual model. We give a new criterion for transparency for a virtual haptic interaction system. This is similar to the transparency of a teleoperation system.¹⁸

The transparency of a virtual haptic interaction system is defined as

$$\Delta = \frac{Z_o}{Z_c} \times 100\% \tag{15}$$

where Z_0 is the impedance presented to the operator and Z_e is the impedance of the virtual model.³ They can be expressed as follows:

$$Z_{\rm o} = \frac{f_{\rm o}}{v_{\rm o}} \tag{16}$$

$$Z_{\rm e} = \frac{f_{\rm e}}{v_{\rm e}} \tag{17}$$

where f_o is the force presented to the operator, v_o is the operator velocity, f_e is the interaction force between the virtual instrument and tissues according to the virtual model, and v_e is the virtual instrument velocity.

The average transparency of the interaction is defined as the average of the transparencies from the first to last sampling instants during the interaction. This can be expressed using equation (18):

$$\bar{\Delta}(\%) = \left(\sum_{k=0}^{n-1} \frac{Z_o}{Z_e}\right) / n \times 100 \tag{18}$$

The transparency illustrates the difference between the impedance of the virtual model and the impedance presented to the operator. It describes the fidelity of a virtual haptic interaction system, allowing discussion of its degree. When the impedance presented to the operator is the same as the impedance of the virtual model, the system is ideal and exhibits a transparency of 100%.

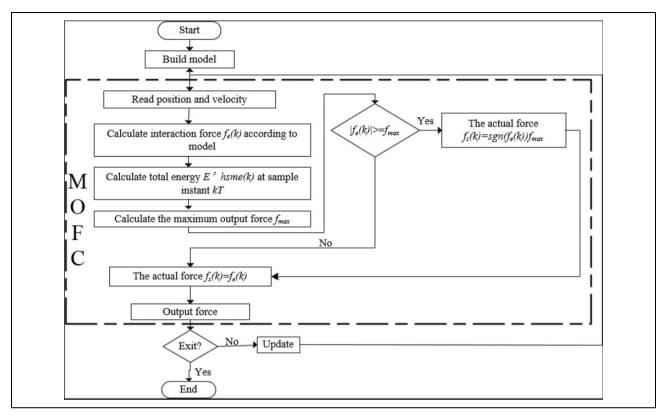


Figure 5. The primary system flow chart.

In order to guarantee virtual interaction system stability, we must limit the output force to the maximum allowable value, which means that the force presented to the operator is sometimes less than that calculated using the virtual model. This decreases the transparency of the virtual interaction system. We have to sacrifice system transparency to improve system stability. What we can do is maximize system transparency with the condition of the guaranteed system stability.

Experimental results

In order to evaluate the MOFC, we performed experiments with the virtual surgery system shown in Figure 4. Because we focus on virtual interaction stability, the task of the operator (surgeon) is to hold the surgical instrument and poke the virtual tissue along an expected trajectory. The expected trajectory of each experiment is a V-like path. For operating convenience, we don't require the expected trajectory in each experiment to be exactly the same. If the actual instrument trajectory is a V-like path, the system is stable, and the operator can hold and move the instrument as expected. When the virtual surgical instrument interacts with virtual tissues, the interaction force between the two is presented to the operator. Three types of virtual tissues were interacted with in this article. The first and second experiments involved interactions with soft tissues and rigid tissues, respectively. The final experiment required interaction with a combination of soft and rigid tissues. Lower sampling frequencies lead to difficulty ensuring haptic interaction system stability. ¹⁹ Thus, we used a very low sampling frequency (50 Hz) for all experiments.

Experiments with soft tissues

We performed soft tissue virtual surgical interaction experiments with and without the MOFC. In both experiments, the stiffness and damping of the virtual soft tissues were k=6 N/m and b=15 Ns/m, respectively. The virtual tissue with this stiffness and damping is as soft as meat. The aim of these two experiments was to prove that the surgical interaction is inherently stable and that the MOFC transmits the unchanged interaction force during soft tissue interactions.

Experiment without the MOFC. First, we performed the soft tissue virtual surgical interaction without the MOFC. We held the manipulator and interacted with the virtual tissues along the expected trajectory (a V-like path). The instrument moved along the V-like path as expected. The actual trajectory and force are shown in Figure 6(a) and (b). For soft tissue interactions, the haptic system without the MOFC is inherently stable.

Experiment with the MOFC. Second, we performed the soft tissue virtual surgical interaction with the MOFC. Again, we held the manipulator and interacted with the virtual

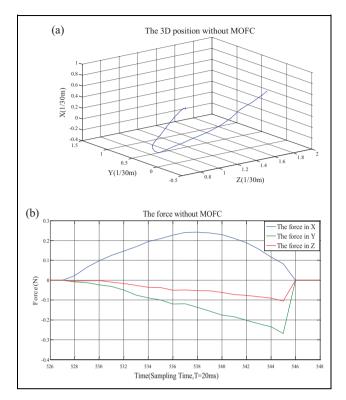


Figure 6. Experiment without the MOFC (k = 6 N/m, b = 15 Ns/m): (a) 3-D position of the surgical instrument and (b) interaction force. MOFC: maximum output force controller; 3-D: three-dimensional.

tissues along the expected trajectory. The actual trajectory and force are shown in Figure 7(a) and (b), respectively. Because the virtual tissue is soft and the virtual interaction system is inherently passive, the MOFC outputs the interaction force calculated using the virtual model to the operator unchanged. Thus, the force before modification in X, Y, and Z is coincident with the force after modification in X, Y, and Z (Figure 7(b)).

From these two experimental results, we can draw the following conclusion: if the virtual tissue stiffness and damping are low (the virtual tissue is soft), it is easy for the virtual surgery system to be passive and the MOFC is not necessary. The MOFC does not play a role in this experiment, and the interaction force is transmitted unchanged. According to equations (15) to (17), the system transparency is 100% for soft tissue interactions.

Experiments with rigid tissues

In this case, we performed rigid tissue virtual surgical interaction experiments with and without the MOFC. In both experiments, the stiffness and damping of the virtual tissues were $k=45\,$ N/m and $b=150\,$ Ns/m, respectively. The tissues are very rigid and feel to the operator like interaction with gristle. The goal of these two experiments was to demonstrate that the virtual surgery system with the MOFC

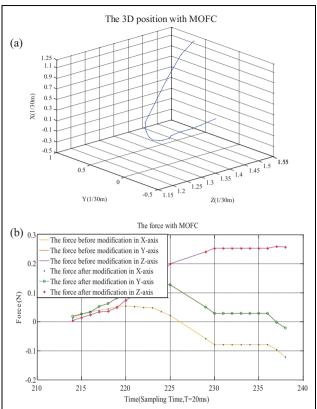


Figure 7. Experiment with the MOFC (k = 6 N/m, b = 15 Ns/m): (a) 3-D position of the surgical instrument and (b) interaction force. MOFC: maximum output force controller; 3-D: three-dimensional.

can maintain stability during rigid interactions, while the system without the MOFC is unstable.

Experiment without the MOFC. First, we performed the rigid tissue virtual surgical interaction without the MOFC. We used the manipulator to poke the virtual tissues along a planned trajectory (a V-like path). Because the virtual tissues are rigid and the output force cannot satisfy the conditions for system passivity, the interaction is not stable. The operator finds that the haptic manipulator does not move as expected. Thus, the instrument trajectory is disturbed and does not follow the V-like path in this case (Figure 8(a)). The interaction force is shown in Figure 8(b).

Experiment with the MOFC. Second, we interacted with the above rigid tissues with the MOFC implemented. Again, we held the manipulator and poked the virtual tissues along the planned trajectory. The actual instrument trajectory is shown in Figure 9(a), and the interaction force is shown in Figure 9(b). Because the MOFC limits the output force, it guarantees that the virtual surgery system is passive. Thus, the 3-D instrument trajectory is not disturbed and the instrument can move smoothly along the V-like path as expected. The force is lower after

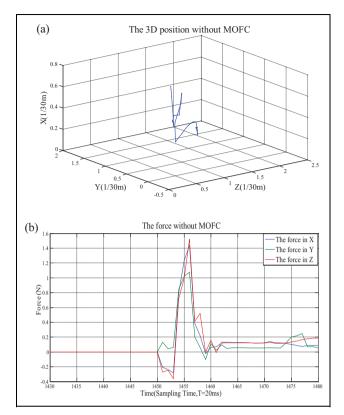


Figure 8. Experiment without the MOFC (k = 45 N/m, b = 150 Ns/m): (a) 3-D position of the surgical instrument and (b) interaction force. MOFC: maximum output force controller; 3-D: three-dimensional.

modification in X, Y, and Z than before from the 649th to the 659th sampling instant (Figure 9(b)). The system stability in this experiment with the MOFC is superior to that in the experiment without the MOFC because the MOFC reduces the output force to the passivity limit. Thus, system transparency is sacrificed. The value of the MOFC is that it outputs the maximum allowable force, which implies that it maximizes system fidelity within the constraint of guaranteed stability. According to the criterion for transparency in the "Definition of transparence for a haptic interaction system" section, the average transparency for the interaction can be calculated using equation (18). The average transparencies in the X, Y, and Z directions are 71.59%, 79.21%, and 73.4%, respectively, during the interaction.

Based on these two experimental results, the MOFC can limit the output force to the maximum value allowed within the constraint of the guaranteed system stability during a rigid interaction. Thus, it can maximize system fidelity with guaranteed stability. This improves system stability by sacrificing the minimum transparency. Tissues that are more rigid lead to more difficulty maintaining system stability. As a result, more force is removed by the MOFC in order to maintain system stability.

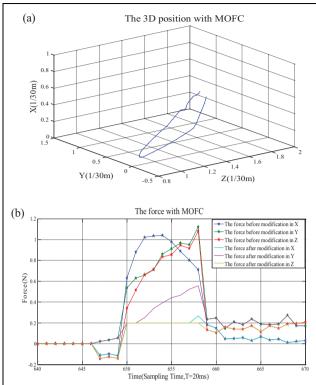


Figure 9. Experiment with the MOFC (k = 45 N/m, b = 150 Ns/m): (a) 3-D position of the surgical instrument, (b) interaction force. MOFC: maximum output force controller; 3-D: three-dimensional.

Experiments with mixed rigid and soft tissues

In real surgery, interactions with an unpredictable mixture of soft and rigid tissues occur. Thus, the controller should be able to adapt to any type of tissue. The aim of this experiment was to prove that the MOFC is a self-adaptive controller for tissues with differing levels of stiffness and damping. We used the manipulator to poke virtual tissues with differing levels of stiffness along the planned trajectory. The soft tissue (k = 6 N/m, k = 15 Ns/m) was poked first, and then the rigid tissue (k = 45 N/m, k = 150 Ns/m) was poked. This experiment was performed with the MOFC.

The actual trajectory is shown in Figure 10(a), and the output force is shown in Figure 10(b). The instrument moves smoothly along the V-like path as expected. When the instrument interacts with the soft tissue, the MOFC does not change the output force. Thus, the forces before and after the MOFC are the same from the 910th sampling point to the 918th sampling point (Figure 10(b)). When the instrument interacts with the rigid tissue, the MOFC limits the output force in order to maintain system stability. Thus, the force after the MOFC is less than the force before the MOFC from the 918th sampling point to the 928th sampling point. This indicates that the MOFC is a self-adaptive

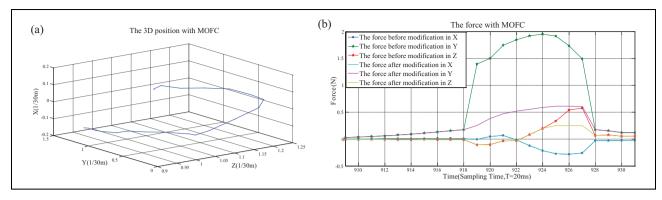


Figure 10. Experiment with the MOFC (k = 6 N/m, b = 15 Ns/m; k = 45 N/m, b = 150 Ns/m): (a) Position of the surgical instrument and (b) interaction force. MOFC: maximum output force controller.

controller. It works well without modification, regardless of the virtual tissue stiffness and damping.

Conclusions

In virtual surgical interactions, virtual tissues can include soft muscles and rigid bones. Maintaining virtual surgical interaction stability can be difficult, especially in the case of rigid interactions. In this work, the MOFC is developed and applied to a virtual surgery system. The MOFC is a self-adaptive controller that can maximize system fidelity within the constraint of guaranteed stability. It works well without modification, regardless of the virtual tissue stiffness and damping. In this article, a new criterion for transparency for a virtual interaction system is presented and it is analyzed for the level of fidelity that the virtual surgery system can achieve in quantity within the constraint of the guaranteed system stability. Because passivity is a sufficient condition for stability, this system is conservative in limiting the output force presented to the operator. This implies that the system fidelity can be further improved using a force controller based on the Lyapunov theorem or other alternatives to the passivity theorem. In the future, we may study less conservative force controllers to achieve better fidelity in virtual surgical operations.

Declaration of conflicting interests

The author(s) declared no potential conflicts of interest with respect to the research, authorship, and/or publication of this article.

Funding

The author(s) disclosed receipt of the following financial support for the research, authorship, and/or publication of this article: This work was partially supported by the National Natural Science Foundation of China under grants 81501560, 61563035, 61662044, 61663027, the Science and Technology Department of Jiangxi Province of China under grants 20171BCB23008, and the hundred people voyage funds from Jiangxi Science and Technology Association.

References

- Burdea GC and Coiffet P. Virtual reality technology, 2nd ed. New York: Wiley-IEEE Press, 2003.
- Zhang X, Sun W, Song A, et al. Virtual lung surgery simulation system based on double-channel haptic interaction. *Chin J Sci Instrum* 2012: 33: 421–427.
- 3. Liu XL and Chen D. Reconstruction of surgical instrument in virtual surgery system. *Int J Mach Learn Cybern* 2014; 5: 225–231.
- 4. Xie Q and Geng G. Fast collision detection method in virtual surgery. *J Comput Info Syst* 2012; 8: 8945–8952.
- Colgate JE, Stanley MC and Brown JM. Issues in the haptic display of tool use. In: 1995 IEEE/RSJ international conference on intelligent robots and systems, Pittsburgh, PA, USA, 5–9 August 1995, pp. 140–145. IEEE
- Adams JR and Hannaford B. A two-port framework for the design of unconditionally stable haptic interfaces. In: 1998 IEEE/RSJ international conference on intelligent robots and systems, Victoria, BC, Canada, 17 October 1998, pp. 1254–1259. IEEE.
- Kim JP and Ryu J. Stable haptic interaction control using energy bounding algorithm. In: 2004 IEEE/RSJ international conference on intelligent robots and systems, Sendai, Japan, 28 September–2 October 2004, pp. 1210–1217. IEEE
- 8. Hannaford B and Ryu JH. Time domain passivity control of haptic interfaces. *IEEE Trans Robot Automat* 2002; 18: 1–10.
- 9. Ryu JH, Preusche C, Hannaford B, et al. Time domain passivity control with reference energy following. *IEEE Trans Control Syst Technol* 2005; 13: 737–742.
- Ryu JH and Yoon MY. Memory-based passivation approach for stable haptic interaction. *IEEE/ASME Trans Mechatron* 2014; 19: 1424–1435.
- Jafari A and Ryu JH. 6-DOF extension of memory-based passivation approach for stable haptic interaction. *Intel Serv Robot* 2015; 8: 23–34.
- 12. Do TH and Ryu JH. Memory based passivation method for stable haptic interaction. In: 2011 IEEE World Haptics

- Conference (WHC), Istanbul, Turkey, 21–24 June 2011, pp. 409–414.
- Han B and Ryu JH. An injecting method of physical damping to haptic interfaces based on FPGA. In: 2008 International Conference on Control, Automation and Systems (ICCAS), Seoul, South Korea, 14–17 October 2008, pp. 1835–1840.
- Kyungno L and Doo YL. Adjusting output-limiter for stable haptic rendering in virtual environments. *IEEE Trans Control* Syst Technol 2009; 17: 768–779.
- Adams JR and Hannaford B. Control law design for haptic interfaces to virtual reality. *IEEE Trans Control Syst Technol* 2002; 10: 3–13.
- Hogan N. Multivariable mechanics of the neuromuscular system. In: *IEEE 8th Annual Conference of the Engineering* in Medicine and Biology Society, Fort Worth, TX, 7–10 November 1986, pp. 594–598.
- Hu LY, Yang YB and Xu SP. Force feedback and control for wave-variable teleoperation systems with time delays. *Int J Robot Autom* 2014; 29: 338–348.
- 18. Lawrence DA. Stability and transparency in bilateral teleoperation. *IEEE Trans Robot Autom* 1993; 9: 624–637.
- 19. Lu X, Zhao H and Ye YQ. Stable haptic rendering using a pipelined threading architecture. *Int J Adv Robot Syst* 2012; 9: 1–6.